

Proceeding Paper

# Mineral Exploration at the Kimmeria Fe-Cu Skarn Deposit, N. Greece: Reassessment and New Perspectives Focusing on the CRMs<sup>†</sup>

Michalis Fitros , Constantinos Mavrogonatos , Marianthi Anastasatou , Adamantia Chatziapostolou, Konstantinos Laskaridis , Petros Karmis, Magdalini Angeli, Dimitrios Tsouvalas, Alexandros Liakopoulos, Dimitrios Tarenidis and Vasiliki Angelatou

Hellenic Survey of Geology and Mineral Exploration, 13672 Acharnae, Greece; m.fitros@igme.gr (M.F.); mavrogon@igme.gr (C.M.); anastasatou@igme.gr (M.A.); achatzia@igme.gr (A.C.); karmis@igme.gr (P.K.); maggeli@igme.gr (M.A.); dtsouvalas@igme.gr (D.T.); aliakopoulos@igme.gr (A.L.); dtar@igme.gr (D.T.); vasaggelatos@igme.gr (V.A.)

\* Correspondence: laskaridis@igme.gr

<sup>†</sup> Presented at the 2nd International Conference on Raw Materials and Circular Economy “RawMat2023”, Athens, Greece, 28 August–2 September 2023.

**Abstract:** Following the worldwide increasing demand for Critical Raw Materials (CRMs), the Hellenic Geological Survey (HSGME) implemented a national project focused on the re-evaluation of certain Public Mining Areas in Greece. In this framework, exploration activities, including geological mapping, and mineralogical, geochemical, and geophysical studies, revealed significant mineralization targets which possibly host elevated contents of certain CRMs in the Kimmeria Fe skarn deposit. The mineralization is related to the contact metamorphic aureole of the Oligocene Xanthi pluton. Various skarn minerals form the following paragenetic zones in order of decreasing temperature: (i) garnet–wollastonite, (ii) garnet–clinopyroxene, (iii) garnet–epidote, and (iv) vesuvianite–scapolite. The skarn deposit consists of magnetite-rich ore occurring along with sulfides (chalcopyrite, pyrite, bismuthinite, and molybdenite), scheelite, minor sulfosalts (aikinite, wittichenite, and cubanite) and native elements (Au and Bi). Bulk-rock geochemical analyses yielded significant values, as follows: Fe<sub>2</sub>O<sub>3</sub>, up to 58 wt%; Cu, up to 6.6 wt%; Bi, up to 1100 ppm; W, up to 670 ppm; V, up to 200 ppm; Mo, up to 200 ppm; and Au, up to 2.1 g/t. Soil and stream sediment geochemistry reveals spatial and linear trends for certain groups of associated elements (i.e., Fe<sub>2</sub>O<sub>3</sub>–Cu–Bi–W and Mo–W–Zn). These trends reflect the surficial distribution of mineralized zones and imply the existence of partially unexposed mineralization in the western part of the study area, a fact also supported by geophysical evidence. A preliminary drilling project has been proposed to evaluate the qualitative characteristics of the deeper parts of the mineralization, investigate buried ore zones in the western part, and overall, reassess the economic potential of the deposit.

**Keywords:** Critical Raw Materials; skarn deposit; exploration; sulfides; ore geology



**Citation:** Fitros, M.; Mavrogonatos, C.; Anastasatou, M.; Chatziapostolou, A.; Laskaridis, K.; Karmis, P.; Angeli, M.; Tsouvalas, D.; Liakopoulos, A.; Tarenidis, D.; et al. Mineral Exploration at the Kimmeria Fe-Cu Skarn Deposit, N. Greece: Reassessment and New Perspectives Focusing on the CRMs. *Mater. Proc.* **2023**, *15*, 75. <https://doi.org/10.3390/materproc2023015075>

Academic Editors: Antonios Peppas, Christos Roumpos, Charalampos Vasilatos and Anthimos Xenidis

Published: 12 January 2024



**Copyright:** © 2024 by the authors. Licensee MDPI, Basel, Switzerland. This article is an open access article distributed under the terms and conditions of the Creative Commons Attribution (CC BY) license (<https://creativecommons.org/licenses/by/4.0/>).

## 1. Introduction

Considering the exponential increase in the worldwide demand for Critical Raw Materials (CRMs) in the coming years, the European Commission has put forward a European Critical Raw Materials Act (COM(2023)160 EU) [1]. In compliance with this framework, all member countries are to implement national strategic plans aiming at the discovery of new CRM-hosting deposits or re-evaluating ore deposits that have been exploited in the past since they may still hold potential for certain CRMs that have not been given proper attention. Accordingly, the Hellenic Survey of Geology and Mineral Exploration (HSGME) implemented a national project focused on the re-evaluation of certain Public Mining Areas in Greece. Exploration activities, i.e., geological mapping, and

mineralogical, geochemical, and geophysical studies that took place at the Kimmeria Fe skarn deposit, Xanthi area, N. Greece, re-evaluated the already known occurrences and revealed promising ore-bearing targets with elevated contents of certain CRMs like Cu, Bi, W, Mo, V, and REEs.

Herein, we present a geological mapping and new mineralogical and geochemical data from the metalliferous zones of the Xanthi Fe skarn. We focus on the CRMs-bearing ore and especially on the elements that have not been economically valued in previous studies, e.g., Bi, Nb, and V.

## 2. Geological Framework

### 2.1. Regional Geology

The Xanthi Fe skarn deposit is located within the Nestos Shear Zone (NSZ), which separates the Rhodopian Units and possibly marks the location of a collapsing thrust wedge [2,3]. In northern Greece, the Rhodope Massif (RM) forms the innermost zone of the Hellenic orogen (e.g., Bonev et al. [4]) and comprises two Alpine nappes (Figure 1): the Lower Tectonic Unit (LTU) comprises ortho- and paragneisses, mica-schists, and amphibolites. These lithologies are overlain by Triassic dolomitic marbles, which are in turn overlain by augen gneisses with Carboniferous to Permian protolith ages [2,3] (Figure 1). The Upper Tectonic Unit (UTU) consists of two petrologically similar subunits but of different protolith and metamorphic ages. The most common lithotypes comprise ortho- and paragneisses, migmatitized gneisses, and migmatites ( $\sim 40.0 \pm 1.0$  Ma by zircon dating [5]), impure marbles, amphibolites, preserved eclogites, and rare meta-mafics or -ultramafics [2,3,6], Figure 1).

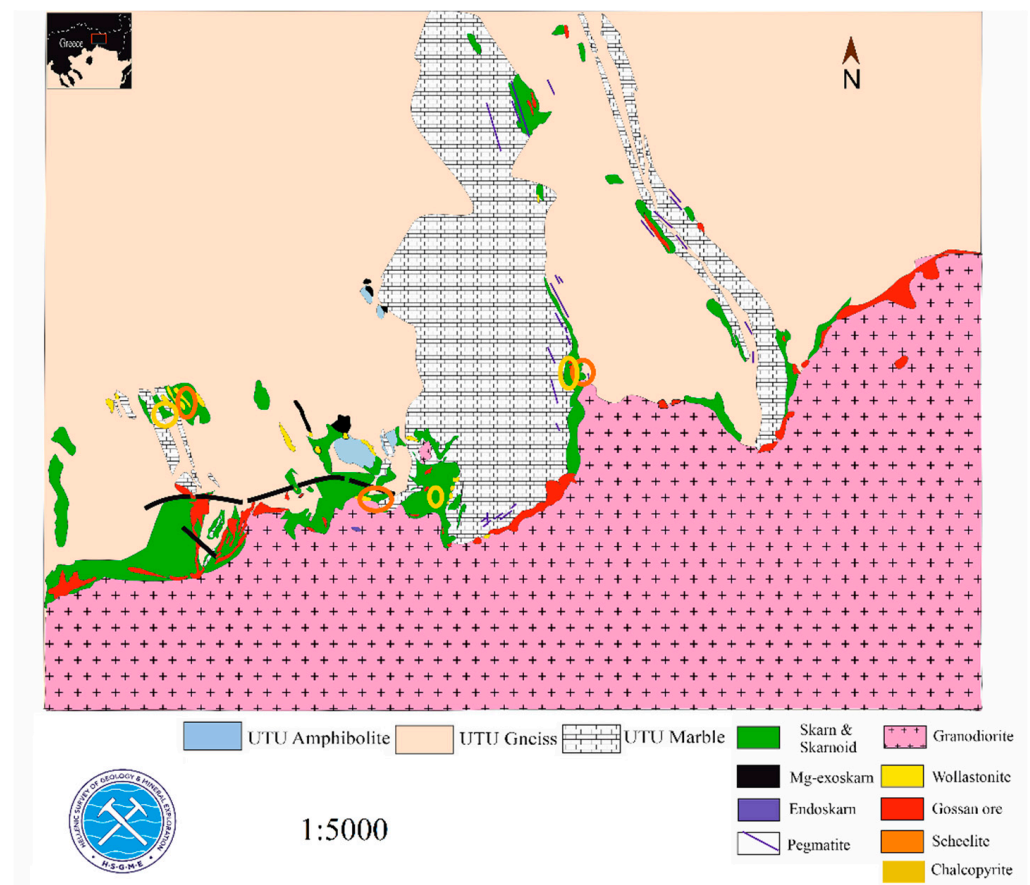


**Figure 1.** Geological map indicating the main skarn zones and related Fe skarn mineralization (modified after [6]).

The two units are divided by the so-called Nestos Shear Zone (NSZ) [3,7]. This tectonic zone comprises a mylonitic, crustal-scale, SW-verging thrust zone (Figure 1). The NSZ footwall lithologies are para- and orthogneisses, intercalated with amphibolites, mica schists, and marbles. On the other hand, migmatitized para- and orthogneisses, impure marbles, retrogressed eclogites, pegmatites, and serpentinized ultramafic rocks comprise the basic lithologies of the NSZ hanging wall. A volcano-sedimentary sequence (VSS) overlies the UTU and consists of sedimentary rocks (e.g., sandstones, marls, limestones, etc.) of Eocene to Oligocene age. Finally, the VSS is locally crosscut by NNW-trending basaltic andesite dykes, dated at  $33.5 \pm 1.2$  Ma [8].

## 2.2. The Xanthi Plutonic Complex

The Xanthi plutonic complex (Figure 1), collectively described as the “granodiorite of Xanthi”, is a laccolith intruding the NSZ. Its emplacement was facilitated by the NE-trending Kavala–Xanthi–Komotini (KXK) normal fault zone under an extensional tectonic regime [2,3,9]. Radiometric dating for the pluton (Figures 1 and 2a) [8,9] yielded ages 34 to 25 ( $\pm 0.5$ ) Ma for the western part and 27 to 25 ( $\pm 0.6$ ) Ma for the eastern part [10–12]. A compositional variation characterizes the intrusive body, with monzonite (and subordinate diorite, monzo-diorite and -gabbro, and even cumulative gabbro) occupying the eastern part (Figure 1) [11,12], while granodiorite to gneissic and porphyritic granite compositions prevail in the western part. At certain places, abundant mafic enclaves ( $Hbl \geq 70$  vol%) and migmatized dioritic xenoliths occur [9]. Finally, zoned pegmatite, rare lamprophyre, haplogranite or aplite, andesite dikes, and quartz veins crosscut both the intrusive body and its host rocks [9] (Figures 1 and 2a).

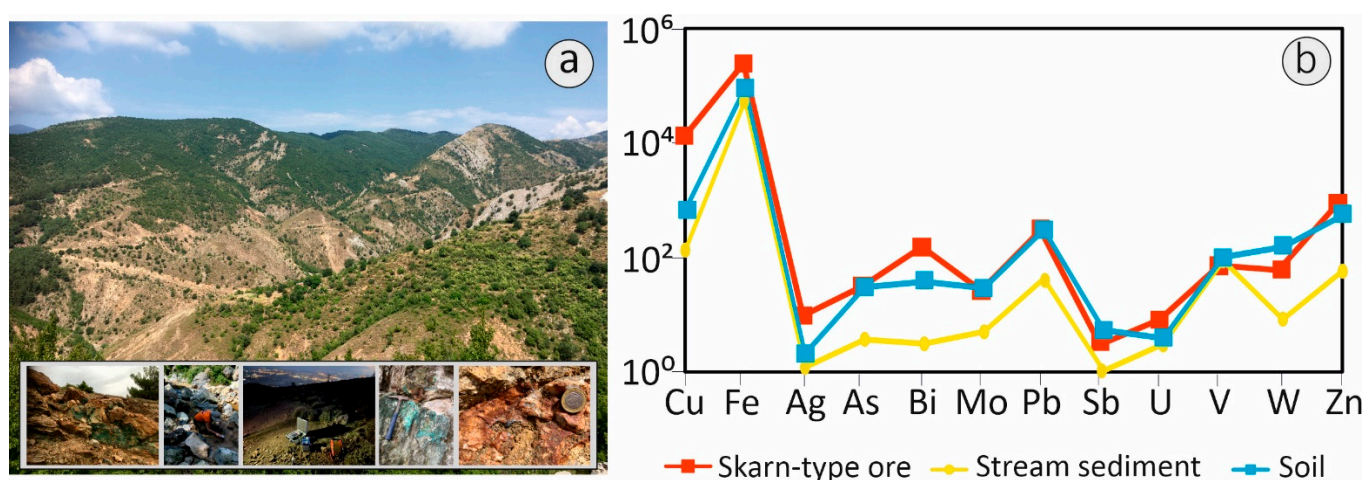


**Figure 2.** (a) Panoramic view of the Fe-Cu skarn deposit at Kimmeria, Xanthi. Inset photos depict various stages of the fieldwork. (b) Geochemical distribution patterns comparing the average abundances of certain elements in skarn-type mineralization, soils, and stream sediments (Fe =  $Fe_2O_3$ ; values in ppm).

## 2.3. The Kimmeria Skarn Deposit

An impressive contact metamorphic aureole reaching in width up to ~400 m, is related to the Xanthi granitoid [13–15] (Figure 1). Skarnoids and hornfelses comprise massive and fine-grained assemblages, replacing gneissic and amphibolitic lithologies of both LTU and UTU rocks. Close to the intrusion, a discontinuous pyroxene–hornfels zone occurs, followed by a distal hornblende-to-biotite hornfels zone.

At certain places, discontinuous and irregular-shaped skarnoids occur adjacent to the hornfelses, reaching a thickness of up to 20 m. Skarns develop along the points of contact of the marbles with the Xanthi pluton (Figure 1) or other minor intrusive phases, e.g., pegmatitic and aplitic dikes and sills. The skarns mainly occur within the UTU [13], LTU, and the VSS rocks (Figure 1). Exoskarns occur as medium-to-coarse-grained

stratabound and contact-controlled bodies. Depending on the composition of the protolith, both Mg- and Ca-skarns occur, with the latter prevailing (Figure 1). Field relations hold evidence that the Ca skarns comprise four succeeding zones with gradual and/or sharp contacts (Figure 2a).

The prograde skarn zones comprise of a pyroxene–garnet zone (Px-Grt) closer to the pluton which evolves into a wollastonite–garnet zone (Wo-Grt) adjacent to the point of contact of the pluton with the marbles. The epidote–garnet (Grt-Ep) zone represents the retrograde stage and usually occurs proximal to the Xanthi's pluton and overprints the other zones. Finally, a discontinuous vesuvianite–scapolite zone (Ves-Scp) occurs at certain places adjacent to the pluton. Metasomatism has locally also affected the Xanthi's granodiorite and monzonite, forming endoskarns, which appear mostly as vertical veins and pipes with widths  $\leq 30$  m and an aplitic texture. Two endoskarn zones are recognized: an inner garnet–epidote zone (Grt-Ep) followed by an outer epidote–orthoclase zone (Ep-Or).

### 3. Materials and Methods

#### 3.1. Petrography and Mineral Chemistry

Skarn gangue and ore minerals were evaluated using scanning electron microscopy (SEM) and energy-dispersive X-ray (EDX) analysis. The analyses were carried out at the Hellenic Survey for Geology and Mineral Exploration (Greece) using a Jeol JSM-IT500 Scanning Electron Microscope instrument (JEOL USA, Inc., Peabody, MA, USA) equipped with an OXFORD 100 Ultramax analytical device (Oxford Inc., Oxford, UK). The operating conditions were a 15 kV accelerating voltage and 3.3 nA beam current with a 4  $\mu\text{m}$  diameter beam. X-ray counts were converted to wt. % oxide using the Cameca PAP correction program.

#### 3.2. Major and Trace Element Geochemical Analysis

Major and trace elements analyses were conducted on a total of 50 bulk ore samples comprising skarn-type mineralization. The geochemical analyses were performed at the Laboratories of HSGME (Athens, Greece) and ActLabs, (Ancaster, ON, Canada).

### 4. Results and Discussion

#### 4.1. Petrography and Mineral Chemistry

The Xanthi's skarn is divided into four main zones: (i) garnet–wollastonite (Grt-Wo), (ii) garnet–clinopyroxene (Grt-Cpx), (iii) garnet–epidote (Grt-Ep), and (iv) vesuvianite–scapolite (Ves-Scp). The Grt-Wo zone comprises fibrous wollastonite crystals, granoblastic-to-poikiloblastic garnet, clear and milky quartz, calcite–dolomite, and minor scheelite, apatite, zircon, titanite, and chlorite. The main ore minerals of this zone are magnetite, pyrite, ilmenite, pyrophanite, and hematite. The Grt-Cpx zone comprises granoblastic-to-poikiloblastic garnet and clinopyroxene (Di-Hd-Bab); scheelite  $\pm$  quartz  $\pm$  calcite  $\pm$  ilvaite; and minor pyrophanite, apatite, epidote, zircon, titanite. The main ore minerals of this zone are pyrite, chalcopyrite, magnetite, pyrrhotite, hematite-goethite, bismuthinite, and molybdenite. The Grt-Ep zone comprises granoblastic-to-poikiloblastic REE-bearing epidote (~70 vol%) and garnet (~20 vol%), as well as clinozoisite, titanite, quartz  $\pm$  albite, adularia, orthoclase, calcite–dolomite, actinolite, biotite, apatite, zircon, and chlorite, with crystal sizes ranging from 0.3 mm to 10 cm. The main ore minerals of this zone are pyrite; hematite; molybdenite; chalcopyrite; molybdenite; and minor aikinite, wittichenite, cubanite, and native elements, i.e., Au and Bi (also [15]). The Ves-Scp zone comprises granoblastic chromium-bearing vesuvianite, scapolite, clinopyroxene (Di-Hd), calcite–dolomite, plagioclase, chlorite, actinolite and minor epidote, muscovite, orthopyroxene, adularia, apatite, and zircon. The main ore minerals of this zone are magnetite, pyrite, and chromite.

To summarize, the skarn zones are associated with magnetite-rich mineralization accompanied by sulfides (chalcopyrite, pyrite, bismuthinite, and molybdenite), scheelite, and minor sulfosalts (aikinite, emplectite, wittichenite, and cubanite) and native elements (Au, Bi, and electrum).

#### 4.2. Geochemical Analyses

Bulk-ore geochemical analyses yielded significant values, as follows: Fe<sub>2</sub>O<sub>3</sub>, up to 58 wt%; Cu, up to 6.6 wt%; Bi, up to 1100 ppm; W, up to 670 ppm; V, up to 200 ppm; Mo, up to 200 ppm; and Au, <2.1 g/t (Table 1). The significant values of iron, copper, bismuth, and tungsten are associated with magnetite-rich mineralization, whereas molybdenum, vanadium, and niobium are related to endoskarn and vein-type mineralization. Native gold and bismuth are mostly related to exoskarn chalcopyrite-rich mineralization. According to soil and stream sediments, geochemistry reveals spatial and linear trends for certain groups of associated elements (i.e., Fe<sub>2</sub>O<sub>3</sub>-Cu-Bi-W and Mo-W-Zn) (Figure 2b). These trends reflect the surficial distribution of mineralized zones and imply the existence of partially unexposed mineralization in the western part of the study area, a fact also supported by geophysical evidence [16].

**Table 1.** Geochemical analyses of selected samples from the Kimmeria Fe skarn deposit.

Elements <sup>1</sup>	Min	Max	Average
Cu	44	65,905	12,764
Fe <sub>2</sub> O <sub>3</sub>	5	83	25
Ag	1	31	10
As	3	160	31
Bi	1	1150	152
Mo	3	200	26
Pb	8	3500	298
Sb	1	12	3
U	1	90	8
V	5	245	72
W	3	310	60
Zn	50	10,000	873

<sup>1</sup> All values are reported in ppm except for Fe<sub>2</sub>O<sub>3</sub> in wt%.

#### 5. Conclusions

The metasomatic evolution of host rocks within the aureole includes three phases. A prograde isochemical metamorphic phase led to the formation of hornfels. This phase was succeeded by a metasomatic phase that formed early skarnoids, followed by calcic exo- and late endoskarns, and a retrograde phase related to their alteration. This metasomatic event resulted in the formation of the Fe skarn ore deposit, which, at certain places, is rich in elements like Cu, Bi, W, Mo, V, and REEs, all of which are of critical importance.

Given the encouraging data from the mineral chemistry and geochemical study, a preliminary drilling project has been proposed to evaluate the quality characteristics of the mineralization's deeper part to investigate and explore buried ore zones in the western part, and finally, to fully reassess the deposit's economic potential. Samples and data analyses are still in progress, and the final trends are expected to be delineated.

Regarding soils and stream sediments, their geochemical patterns follow skarn-type mineralization, and soils highlight the area's potential in CRMs, such as Cu, W, and Bi (Figure 2b). Moreover, geochemical spatial trends of soils emphasize the considerable presence of Fe-Cu-Bi in the western part, and of Mo-W in the eastern part of the study area.

**Author Contributions:** K.L., P.K. and A.L. designed the project; M.F., C.M. and A.C. performed the SEM-EDS analyses; M.A. (Marianthi Anastasatou), C.M., M.F., A.C., V.A., D.T. (Dimitrios Tarenidis), M.A. (Magdalini Angeli) and D.T. (Dimitrios Tsouvalas) performed the geochemical analyses. All authors contributed to the interpretation and performed comprehensive editing. All authors have read and agreed to the published version of the manuscript.

**Funding:** This research was funded by DYOPY-OPYGEK—Public Mining Area Kimmeria Xanthi/NSRF 2014-2020.

**Institutional Review Board Statement:** Not applicable.

**Informed Consent Statement:** Informed consent was obtained from all subjects involved in the study.

**Data Availability Statement:** Data sharing is not applicable to this article.

**Acknowledgments:** D. Sgouros, V. Spiropoulos, and A. Kirmizopoulos are kindly thanked for providing valuable help during the fieldwork; N. Xirokostas, K. Vallianatou, M. Sakalis, and A. Exikis are thanked for assisting with laboratory work and analyses. Two reviewers are kindly thanked for providing helpful comments that improved the manuscript.

**Conflicts of Interest:** The authors declare no conflicts of interest.

## References

1. COM(2023)160 EU. Proposal for a Regulation Establishing a Framework for Ensuring a Secure and Sustainable Supply of Critical Raw Materials. *Critical Raw Materials Act (CRM Act)*, 16 March 2023.
2. Krenn, K.; Bauer, C.; Proyer, A.; Klotzli, U.; Hoinkes, G. Tectonometamorphic evolution of the Rhodope orogen. *Tectonics* **2010**, *29*, 1–25. [[CrossRef](#)]
3. Nagel, T.J.; Schmidt, S.; Janák, M.; Froitzheim, N.; Jahn-Awe, S.; Georgiev, N. The exposed base of a collapsing wedge: The Nestos shear zone (Rhodope Metamorphic Province, Greece). *Tectonics* **2011**, *30*, 1–17. [[CrossRef](#)]
4. Bonev, N.; Marchev, P.; Moritz, R.; Collings, D. Jurassic subduction zone tectonics of the Rhodope Massif in the Thrace region (NE Greece) as revealed by new U–Pb and <sup>40</sup>Ar/<sup>39</sup>Ar geochronology of the Evros ophiolite and high-grade basement rocks. *Gondwana Res.* **2015**, *27*, 760–775. [[CrossRef](#)]
5. Liati, A.; Gebauer, D. Constraining the prograde and retrograde P–T–t path of Eocene HP-rocks by SHRIMP dating of different zircon domains: Inferred rates of heating, burial, cooling and exhumation for central Rhodope, northern Greece. *Contrib. Mineral. Petrol.* **1999**, *135*, 340–354. [[CrossRef](#)]
6. Liati, A.; Gebauer, D.; Fanning, C.M. Geochronology of the Alpine UHP Rhodope Zone: A Review of Isotopic Ages and Constraints on the Geodynamic Evolution. In *Ultrahigh-Pressure Metamorphism: 25 Years after the Discovery of Coesite and Diamond*; Elsevier Inc.: Amsterdam, The Netherlands, 2011; pp. 295–324.
7. Barr, S.R.; Temperley, S.; Tarney, J. Lateral growth of the continental crust through deep level subduction-accretion: A re-evaluation of central Greek Rhodope. *Lithos* **1999**, *46*, 69–94. [[CrossRef](#)]
8. Eleftheriadis, G.; Christophidis, G.; Kassoli-Fournaki, A. Geochemistry of the high-K calc-alkaline basaltic sills and dykes in the South Rhodope Massif (N. Greece). *Bull. Volcanol.* **1984**, *47*, 569–579. [[CrossRef](#)]
9. Koukouvelas, I.; Pe-Piper, G. The Oligocene Xanthi pluton, Northern Greece: A granodiorite emplaced during regional extension. *J. Geol. Soc. Lond.* **1991**, *148*, 749–758. [[CrossRef](#)]
10. Bigazzi, N.S.G.; Christofides, G.; Del Moro, A.; Kyriakopoulos, K. A contribution to the evolution of the Xanthi pluton (Northern Greece): The apatite fission track analysis. *Bull. Della Soc. Geol. Ital.* **1994**, *113*, 243–248.
11. Christofides, G.; Papadopoulou, L.; Soldatos, T.; Koroneos, A. Crystallization conditions of the Xanthi plutonic complex (Rhodope Massif, N. Greece): Geothermometry and geobarometry. In Proceedings of the XIX CBGA Congress, Thessaloniki, Greece, 23–26 September 2010; Special Volume 99, pp. 199–207.
12. Christofides, G.; Pipera, K.; Koroneos, A.; Papadopoulos, A. New geochronological data from the Xanthi pluton: Constraints on the Nestos thrust dating. In Proceedings of the School of Prof. Zhivko Ivanov, International Conference: Exhumation of High-Grade Metamorphic Rocks (MCC), Magmatic Arc Systems and Strike-Slip Zones, Sofia, Bulgaria, 29–30 March 2012; pp. 49–52.
13. Liati, A. Regional Metamorphism and Overprinting Contact Metamorphism of the Rhodope Zone, near Xanthi (N. Greece): Petrology, Geochemistry, Geochronology. Ph.D. Thesis, Technische Universität Braunschweig, Braunschweig, Germany, 1986; p. 186.
14. Voudouris, P.; Xinou, A.; Kanellopoulos, C.; Kati, M.; Mavrogonatos, C.; Lyberopoulos, P. A new occurrence of pyrophanite from the amphibolite-hosted skarn in western Kimmeria, Xanthi, Northern Greece. *Bull. Geol. Soc. Greece* **2013**, *47*, 487–496. [[CrossRef](#)]
15. Fitros, M.; Tombros, S.F.; Kokkalas, S.; Kiliass, S.P.; Perraki, M.; Skliros, V.; Simos, X.; Pappaspyropoulos, K.; Avgouropoulos, G.; Williams-Jones, A.E.; et al. REE-enriched skarns in collisional settings: The example of Xanthi’s Fe-skarn, Rhodope Metallogenetic Massif, Northern Greece. *Lithos* **2020**, *370–371*, 105638. [[CrossRef](#)]
16. Karmis, P.; Angeli, M.; Tsouvalas, D.; Mavrogonatos, C.; Fitros, M.; Anastasatou, M.; Chatziapostolou, A.; Laskaridis, K. The Controlled-source Audio-frequency Magnetotellurics (CSAMT/AMT) method tested in the search for deep Fe-Skarn mineralization at Kimmeria, Xanthi, N. Greece. In Proceedings of the RAWMAT 2023—2nd International Conference on Raw Materials and Circular Economy, Athens, Greece, 28 August–2 September 2023.

**Disclaimer/Publisher’s Note:** The statements, opinions and data contained in all publications are solely those of the individual author(s) and contributor(s) and not of MDPI and/or the editor(s). MDPI and/or the editor(s) disclaim responsibility for any injury to people or property resulting from any ideas, methods, instructions or products referred to in the content.